JOURNAL OF CATALYSIS 78, 77–87 (1982)

Characterization of Thin Crystalline Alumina Supports Prepared by Electron Irradiation

A. RENOU

Laboratoire de Microscopie et Diffraction Electroriques, Equipe de Recherche Associée au C.N.R.S. No. 545, Faculté des Sciences et Techniques, Université d'Aix-Marseille III, Rue H. Poincaré, 13397 Marseille Cédex 13, France

Received January 13, 1982; revised June 4, 1982

Thin crystalline alumina supports ("substrates") were produced by electron irradiation of amorphous films in an electron microscope. The resulting alumina structures have been characterized by transmission electron microscopy and transmission electron diffraction. The results show that the structure of alumina is dependent on irradiation conditions. A low irradiation energy leads to 2000-Å-sized grains consisting of η- and/or γ- and δ-Al_2O_3 whilst high irradiation energy yields micron-sized [0001]-, [11$\bar{2}$0]-, and [21$\bar{3}$2]-oriented α-Al_2O_3 (sapphire) grains. These α-Al_2O_3 substrates were used to study the structure of Au and Pd particles condensed on (0001) and (11$\bar{2}$0) areas at a temperature lower than 500°C. When the substrate temperature is between 400 and 500°C, the tetrahedral shape of the particles is influenced by the symmetry of the (0001) substrate but the particles have no azimuthal orientation.

INTRODUCTION

Previous studies of fundamental mechanisms of heterogeneous catalysis have shown that the size, morphology, and structure of the particles of metal catalysts can be in some cases related to their adsorption properties, activity, or selectivity (*1, 2*). To elucidate these relations, systematic studies of the growth of metals deposited on alumina supports (referred to here as "substrates") were undertaken (*3a, 3b*). For this purpose it is necessary to produce clean electron-transparent crystalline substrates because the growth, morphology, and structure of aggregates are dependent on the cleanliness and surface structure of the substrate (*4*).

In this paper, we investigate the morphology and structure of thin crystallized alumina films produced by electron irradiation of amorphous Al_2O_3 films and their use as supports for the growth of Au and Pd particles.

EXPERIMENTAL

Method of preparation. The crystallization process effected by electron irradiation of a specimen is currently used to produce crystalline semiconducters such as Se (*5*) or rare earth oxides (*6*) or sapphire (*7*). A bulk sapphire crystal is evaporated from an electron beam source inside an ultrahigh-vacuum chamber under a vacuum of about 10^{-8} Torr. The thickness of the films condensed onto a NaCl substrate at room temperature is in the range of 200–600 Å. The deposition rate is controlled by a quartz microbalance; it is about 3 Å/s. The samples are stripped from the substrate in water and mounted on a copper grid of a conventional specimen holder of a Siemens Elmiskop 101 microscope. The films have an amorphous struc-

0021-9517/82/110077-11$02.00/0

ture; they are unstable and break under the electron beam if their thickness is less than 200 Å. Samples with a thickness of more than 200 Å were irradiated by intense electron beam flash heating and crystallization then occurred.

Electron microscopy. After their irradiation, the films were analysed by transmission electron microscopy and transmission electron diffraction. It will be shown that the structure of the crystalline films depends on preparation conditions, chiefly those concerned with irradiation energy such as high-voltage electron beam intensity, irradiation time, and localization of the irradiated area with respect to a bar of the grid. In order to produce sufficient beam intensity for crystallization to be induced the electron microscope requires operation with minimum or zero excitation of the first condenser while altering the second condenser lens to produce a focussed spot on the specimen. Typical preparation conditions are high voltage (100 kV) with electron beam diameter, current density, and irradiation time of the flash in the ranges 10–30 μm, 10 mA/cm²–1 A/cm², and 0.25–2 s, respectively.

When the crystallization proceeds under maximum irradiation conditions (100 kV, 1 A/cm², 0.25 s) the specimen generally exhibits three different zones as shown schematically in Fig. 1:

(a) a circular zone labelled A with a diameter in the range of 5–15 μm including long monocrystalline areas such as A_1, A_2, A_3 seen in Fig. 2 with a width ranging between 1.5 and 4 μm and bent contours;

(b) two polycrystalline zones B_1 and B_2 surrounding zone A with small crystals with a mean size of 100 Å;

(c) an amorphous zone C against zone B_2 localized in the vicinity of the bars of the grid.

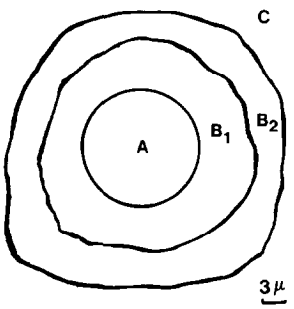

FIG. 1. Diagram indicating the relative positions of recrystallized Al_2O_3 zones on a copper grid. Zone A: monocrystalline; B_1 and B_2: polycrystalline; C: amorphous.

RESULTS AND DISCUSSION

Recrystallized Films

Figures 3a–c show electron diffraction patterns which were frequently observed from selected monocrystalline areas A_1, A_2, and A_3, respectively, and Figs. 3d and e show patterns from polycrystalline areas B_1 and B_2.

(1) Structure of regions B_1 and B_2. The electron diffraction patterns in Figs. 3d and e show that regions B_1 and B_2 have a different polycrystalline structure. The diffraction patterns were calibrated against monocrystalline gold films and the measured d_c spacings compared with known Al_2O_3 structure (*8*). The results are summarized in Tables 1 and 2.

From the comparison between our results and literature data (*8*) it is concluded that the structure of sample B_1 is polycrystalline tetragonal δ-Al_2O_3 and B_2 is polycrystalline η-Al_2O_3 and/or γ-Al_2O_3 spinel. The results listed in Table 2 show that the spacings of planes d and intensities I of the reflections of η-Al_2O_3 and γ-Al_2O_3 are very similar. The principal difference between η- and γ-Al_2O_3 phases is that the (400) and (440) reflections of γ-Al_2O_3 are doubled while those of η-Al_2O_3 have only an asymmetrical profile (*8*). Thus for a fine characterization of sample B_2 the line profiles must be taken into account and for that purpose it is necessary to analyse precisely the shape and position of the diffraction profiles from densitograms. From analysis of direct intensity profiles of electron diffraction patterns of type 3e, the exact nature of

TABLE 1

d Spacings of δ-Al_2O_3 for Sample B_1

d_c (Å)	1.399	1.520	1.616	1.686	1.996	2.295	2.468	2.608	2.894	3.249	4.050	5.100
δ-Al_2O_3[a] *d* (Å)	1.396	1.517	1.604	1.628	1.986	2.279	2.460	2.601	2.881	3.230	4.070	5.100

[a] Data from Lippens and Steggerda (*8*).

sample B_2 could not be concluded. We have noticed on the one hand that samples B_1 and B_2 could be directly produced by electron irradiation of the amorphous phase if a low irradiation beam intensity of the specimen is chosen (condenser aperture removed) (15 and 10 μA, respectively). On the other hand, we have seen that the size of the crystals could increase with increasing irradiation time. In that way it is possible to produce η- and/or γ- or δ-Al_2O_3 grains with a size of about 2000 Å as shown in Fig. 4.

(*2*) *Structure of regions A_1, A_2 and A_3.* Electron diffraction patterns in Figs. 3a–c show that the monocrystalline regions A_1, A_2, and A_3 have a different orientation with respect to the electron beam. As previously, the diffraction patterns were calibrated against polycrystalline gold films and the measured d_c spacings compared with known Al_2O_3 structures (*8*). The data are summarized in Table 3.

From the comparison between our results and literature data (*8*) it is concluded that samples A_1, A_2, and A_3 have the same pseudohexagonal or rhombohedral sapphire structure α-Al_2O_3. We have noticed that it is possible to produce monocrystalline α-Al_2O_3 samples directly by electron irradiation of polycrystalline samples of type B_1 or B_2 under the same preparation conditions as described in the Experimental section. Thus from irradiation of several parts of these samples of 100-μm size large monocrystalline α-Al_2O_3 areas can be prepared. It appears that a subsequent irradiation of these areas has no effect on their

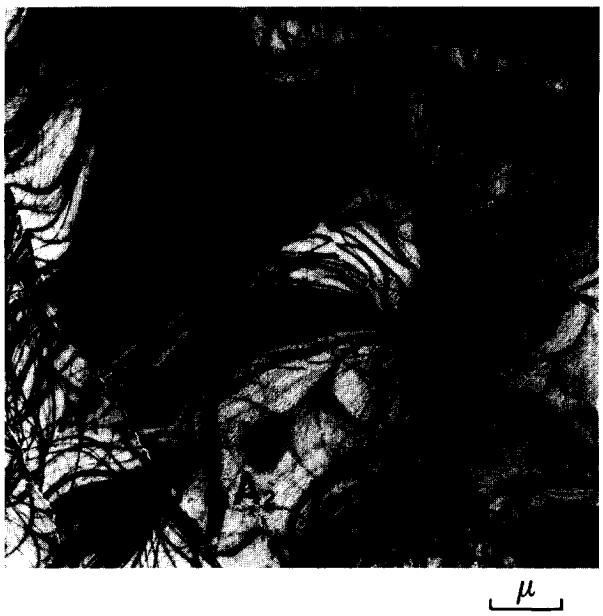

FIG. 2. Electron beam-recrystallized monocrystalline Al_2O_3 areas.

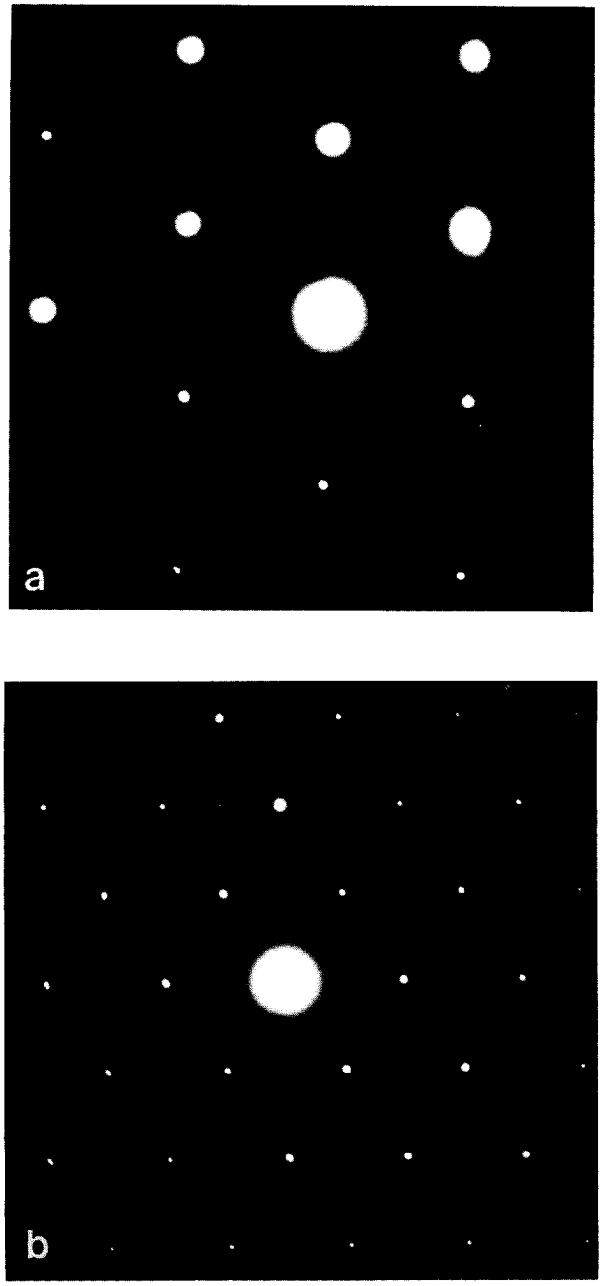

FIG. 3. Electron diffraction patterns from selected monocrystalline areas of samples A_1, A_2, and A_3 oriented (a) (0001), (b) $(11\bar{2}0)$, and (c) $(21\bar{3}2)$ respectively and from selected polycrystalline areas of samples B_1 and B_2; (d) δ-Al_2O_3 and (e) η- and/or γ-Al_2O_3, respectively.

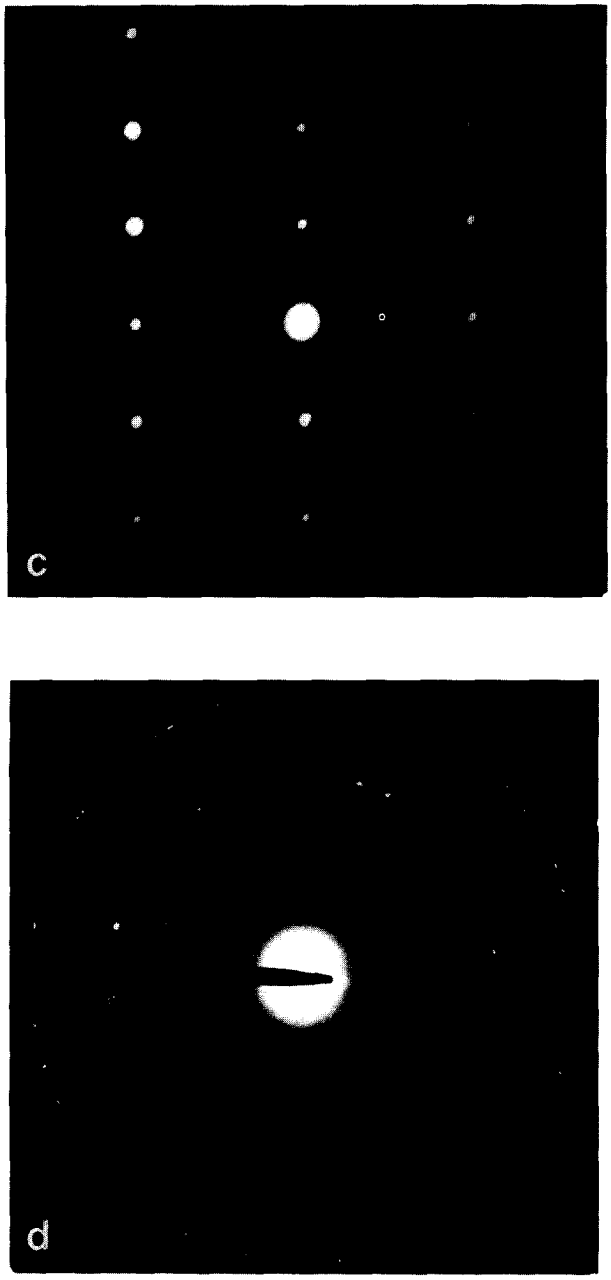

FIG. 3—*Continued.*

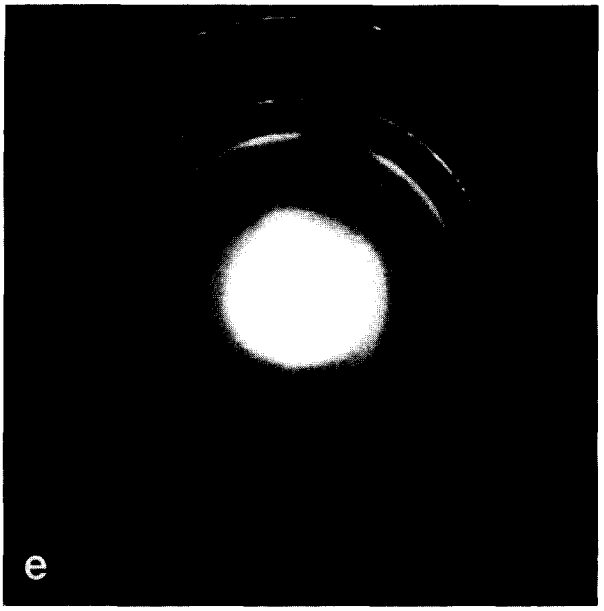

FIG. 3—*Continued.*

nature and their size. From the indexing of electron diffraction patterns (Figs. 3a–c) we conclude that the orientations of samples A_1, A_2, and A_3 are respectively (0001), $(11\bar{2}0)$, and $(21\bar{3}2)$. Generally (0001)- and $(11\bar{2}0)$-oriented monocrystalline areas are frequently observed. Thus after the irradiation of the amorphous film, a temperature gradient exists between the vicinity of the grid bar (cold zone) and the irradiated-region center (hot zone); this is the reason for the formation of the different phases of alumina with the following sequence: amorphous → η and/or γ → δ → α-Al_2O_3.

The results are in agreement with those of Lippens and Steggerda (*8*) about the formation of these phases from the calcination of aluminium hydroxides (boehmite) at different temperatures, e.g.,

$$\text{boehmite} \xrightarrow{350°C} \gamma \xrightarrow{750°C} \delta \xrightarrow{1200°C} \alpha\text{-}Al_2O_3.$$

TABLE 2

d Spacings and Relative Intensities of η- and γ-Alumina for Sample B_2

d_c (Å)	η-Al_2O_3[a] *d* (Å)	*I*	γ-Al_2O_3[a] *d* (Å)	*I*	hkl spinel
4.564	4.57	16	4.6	12	111
2.760	2.76	33	2.77	25	220
2.397	2.395	70	2.397	60	311
2.282	2.284	36	2.284	33	222
1.978	1.980	70	1.990 1.956	65	400
1.521	1.519	16	1.520	15	333/511
1.396	1.396	100	1.407 1.395	100	440

[a] Data from Lippens and Steggerda (*8*).

Recrystallized Areas

Generally, the observation of different parts of monocrystalline α-Al_2O_3 areas shows a particular surface relief strongly marked by contrast effects which differ from one part to another. Different aspects frequently observed are geometrical figures of growth in grains oriented (0001) (Fig. 5a) or straight parallel lines in grains oriented $(11\bar{2}0)$ (Fig. 5b); the distance between these lines is in the range of 250–300 Å. These contrast effects appear distinctly on defocussed images. They have also been observed in lamellar Sm_2O_3 crystals and interpreted as Fresnel fringes produced by parallel and regular terraces limited by

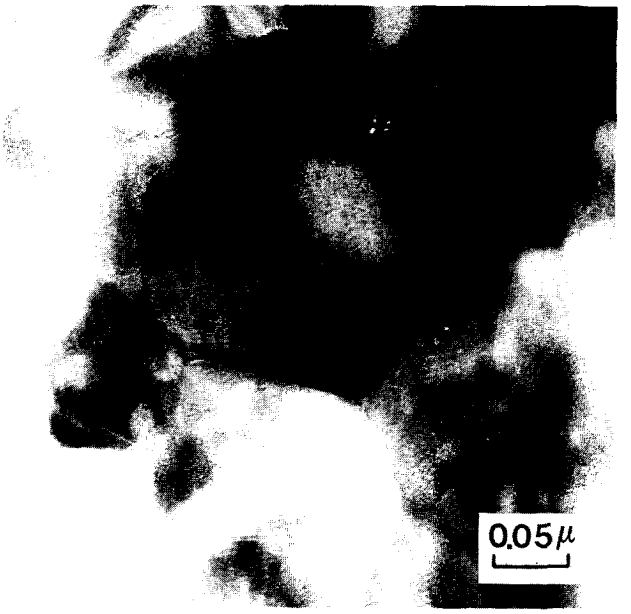

FIG. 4. Large-size recrystallized δ-Al_2O_3 grains.

steps (*9*). For any orientation of the grains, many voids with a size in the range of 200–500 Å are observed; they are randomly distributed in the material or into grain boundaries (Fig. 5c).

The voids appear similar to those frequently formed in quenched and high-temperature annealed alloys. It is generally assumed (*10*) that their formation mechanism is nucleation and growth of thermal vacancies.

Particles Condensed on Recrystallized Monocrystalline Sapphire Supports

Metal vapor deposition on recrystallized sapphire substrates is performed inside a high-vacuum chamber under a vacuum of 10^{-8} Torr. The evaporation is realized on (0001) and (11$\bar{2}$0) 2-μm-sized monocrystalline areas. Before deposition, the substrate is preheated for 30 min at a temperature of about 300°C. During the condensation, the

TABLE 3

d Spacings of α-Al_2O_3 for Samples A_1, A_2, and A_3

A_1	d_c (Å)	2.389		1.384					
	α-Al_2O_3[a] *d* (Å)	2.379		1.373					
A_2	d_c (Å)	3.474	2.360	2.069	1.957	1.724	1.549	1.416	1.380
	α-Al_2O_3[a] *d* (Å)	3.479	2.379	2.085	1.964	1.739	1.546	1.404	1.373
A_3	d_c (Å)	2.378	2.040	1.939	1.503				
	α-Al_2O_3[a] *d* (Å)	2.379	2.085	1.964	1.511				

[a] Data from Lippens and Steggerda (*8*).

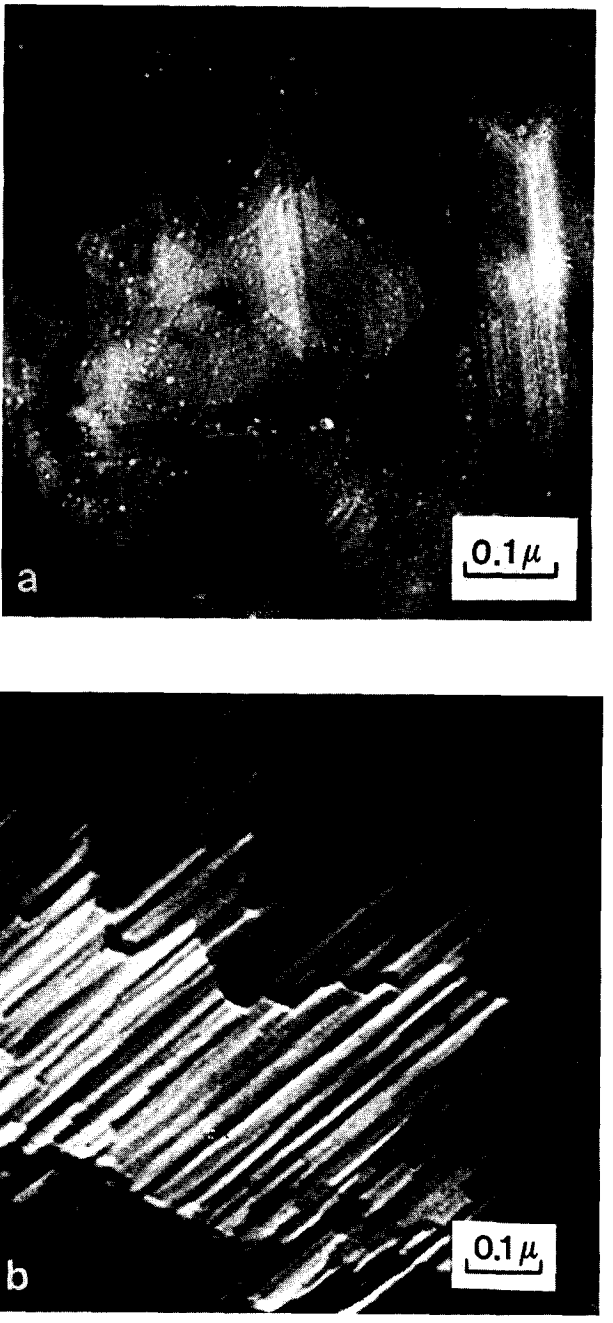

FIG. 5. Monocrystalline α-Al_2O_3 areas exhibiting (a) surface steps in (0001)-oriented grain, (b) surface steps in $(11\bar{2}0)$-oriented grain, (c) voids distributed randomly and in grain boundaries.

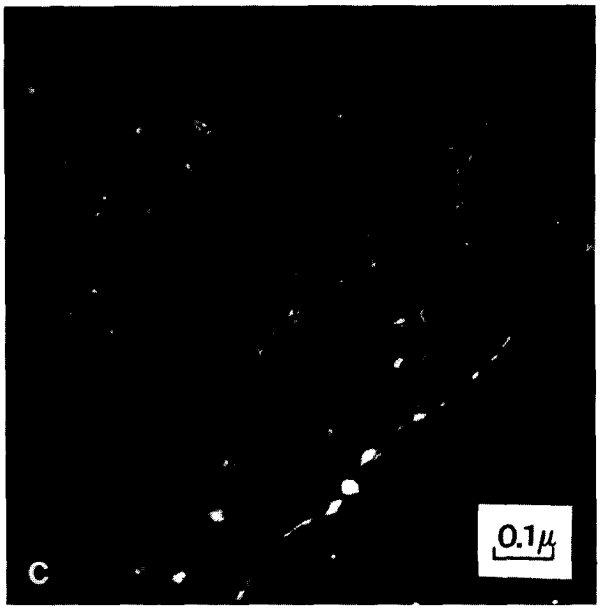

FIG. 5—*Continued.*

substrate temperature is in the range of 200–500°C; the evaporation rate is 10 Å/min and the mean size of the particles is in the range of 30–120 Å.

For gold and palladium deposits produced on (0001)- and $(11\bar{2}0)$-oriented α-Al_2O_3 grains at substrate temperatures (T_s) between 200 and 400°C, electron diffraction patterns exhibit rings which define a polycrystalline structure without azimuthal orientation, as shown in Fig. 6; for any oriented grain, particles do not exhibit particular habits. When the substrate temperature is between 400 and 500°C, on (0001)-oriented grains the morphology of many crystallites is influenced by the symmetry of the (0001) crystal face because of triangular outlines as shown in Fig. 7. The contrasts of these particles show that they have a tetrahedral shape with (111) Pd // (0001) α-Al_2O_3. However, the electron diffraction pattern does not show distinctly either a (111) texture, e.g., a preferential orientation of (111) face, or an azimuthal orientation. We think that under our imaging conditions it is explained by using a large-area selected aperture from which the diffraction pattern was formed. We have noticed that the crystal habits of Au and Pd particles are much less pronounced on $(11\bar{2}0)$-oriented grains. These observations show that under our deposition conditions, no epitaxial gold and palladium particles are obtained. These results are different from those concerning *in situ* deposits onto

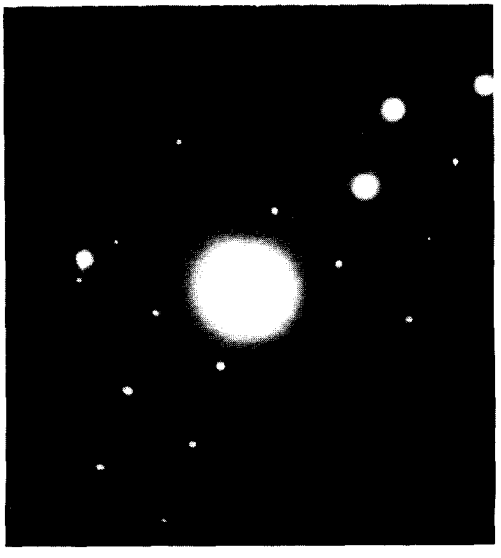

FIG. 6. Electron diffraction pattern from palladium particles deposited onto $(11\bar{2}0)$ α-Al_2O_3; 200°C < T_s < 400°C.

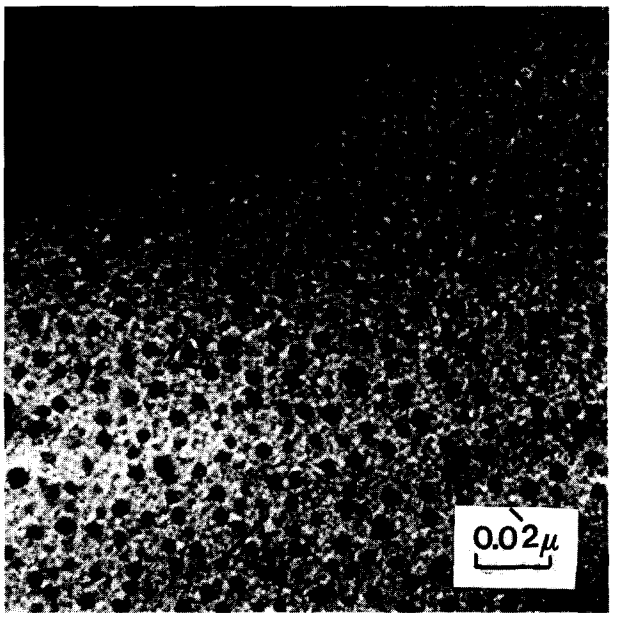

FIG. 7. Palladium particles with triangular outlines grown at 500°C on (0001) recrystallized α-Al_2O_3 grains. Evaporation rate: 10 Å/min.

(0001) recrystallized monocrystalline α-Al_2O_3 at a substrate temperature of 750°C where particles nucleate epitaxially (*3b*). In our case, the lack of any substrate effect on azimuthal orientation of the particles is probably explained by contamination of the substrate before deposition and the low temperature of the substrate during the condensation.

CONCLUSIONS

The formation of different structures of recrystallized Al_2O_3 from electron flash heating of amorphous alumina films is a consequence of different irradiation conditions of the alumina. A low-energy irradiation of the amorphous film leads to δ-Al_2O_3, η-Al_2O_3, and/or γ-Al_2O_3 polycrystalline structures of 2000-Å grain size, while a high-energy irradiation of amorphous or polycrystalline films leads to 100-μm-size large monocrystalline α-Al_2O_3 areas with (0001) $(11\bar{2}0)$ $(21\bar{3}2)$-oriented grains of about 1-μm size. Thus modification of the irradiation conditions of the electron beam allows one to control the structure and grain size. Such well-defined substrates prepared with high reproducibility are suitable for nucleation and growth studies of small metallic particles.

Initial observations of the morphology and structure of gold and palladium particles condensed onto an α-Al_2O_3 monocrystalline substrate at a temperature between 400 and 500°C show that many of them have a tetrahedral shape with a preferential orientation of (111) faces onto the substrate, e.g., (111) Pd parallel to (0001) α-Al_2O_3. However, these particles have no azimuthal orientation.

REFERENCES

1. Maat, M. J., and Moscou, L., *in* "Proceedings, 3rd International Congress on Catalysis, Amsterdam, 1964," p. 1276. North-Holland, Amsterdam, 1965.
2. Barron, Y., Maire, G., Cornet, D., Muller, J. M., and Gault, F. G., *J. Catal.* **2**, 152 (1963); **5** 428 (1966).
3. (*a*) Poppa, H., Lee, E. H., and Moorhead, R. D.,

J. Vac. Sci. Technol. **15,** 1100 (1978); (*b*) Anton, R., Poppa, H., and Heinemann, K., *in* "Proceedings, EMSA Atlanta (1981)," in press.
4. Renou, A., and Gillet, M., *Thin Solid Films* **41,** 15 (1977).
5. Ogura, I., and Nagashima, S., *in* "Proceedings, 8th Intern. Vac. Congress, Cannes, 1980," p. 141.
6. Portier, R., Fayard, M., Boulesteix, O., and Caro, P. E., *Mater. Res. Bull.* **8,** 693 (1973).
7. Heinemann, K., Anton, R., and Poppa, H., *in* "Proceedings, EMSA Atlanta (1981)," in press.
8. Lippens, B. C., and Steggerda, J. J., "Physical and Chemical Aspects of Adsorbents and Catalysts." Academic Press, New York, 1970.
9. Boulesteix, C., Colliex, C., Mory, C., Renard, D., and Yangui, B., *J. Microsc. Spectrosc. Electron.* **3,** 185 (1978).
10. Epperson, J. E., Gerstenberg, K. W., Berner, D., Kostorz, G., and Ortiz, C., *Philos. Mag. Part A* **38,** 529 (1978).